Supporting Information

LCST Ion Gels Fabricating "all-in-one" Smart Windows: Thermotropic, Electrochromic and Power Generating

Yue Ma[1], Yunbo Wang[1], Junyu Zhou[1], Yueyang Lan[1], Sheng Jiang[1], Yifan Ge[1], Shuai Tan[1], Shiguo, Zhang[2], Caihong Wang[1], Yong Wu[1]*

[1] School of Chemical Engineering, Sichuan University, Chengdu 610065, China

[2] College of Materials Science and Engineering, Hunan University, Changsha 410004, China

1 Synthesis

1.1 Materials

n-Butyl acrylate (BA), poly(ethylene glycol) diacrylate, and 1-ethyl-3-methylimidazolium bis(trifluoromethylsulfonyl)imide were directly utilized as purchased from Meryer (Shanghai) Chemical Technology Co., Ltd. Photoinitiator, 1-hydroxycyclohexyl phenyl ketone, was purchased from Shanghai Adamas Reagent Co., Ltd. The polymerization was conducted at ambient without extra removing of air or oxygen.

1.2 Polymerization of the PBA ion gel.

At room temperature, BA (1.2 g, 9.4 mmol) and poly(ethylene glycol) diacrylate (3.6 mg, 0.03 mmol) were firstly dissolved in 1-ethyl-3-methylimidazolium bis(trifluoromethylsulfonyl)imide (0.8 g, 2.0 mmol). Then photoinitiator of 1-hydroxycyclohexyl phenyl ketone (12 mg, 0.03 mmol) was added with strongly stirring to obtain a transparent and colorless solution. The polymerization of the mixtures was conducted under UV irradiation for 30 mins at ambient to produce thermoresponsive PBA ion gels.

1.3 Polymerization of the non-thermoresponsive ion gel.

At room temperature, methyl methacrylate (1.2 g, 12 mmol) and poly(ethylene glycol) diacrylate (3.6 mg, 0.03 mmol) were firstly dissolved in 1-ethyl-3-methylimidazolium bis(trifluoromethylsulfonyl)imide (0.8 g, 2.0 mmol). Then photoinitiator of 1-hydroxycyclohexyl phenyl ketone (12 mg, 0.03 mmol) was added with strongly stirring to obtain a transparent and colorless solution. The polymerization of the mixtures was conducted under UV irradiation (380 nm, 100 mW/cm^2) for 30 mins at ambient to produce non-thermoresponsive ion gels.

1.4 Fabrication of PBA ion gel-based smart window.

Firstly, the monomer mixture was sandwiched by two ITO glasses and then conducted in situ polymerization under UV irradiation for 30 mins. The size of the ion gel in smart window was 5 cm×5 cm with a thickness of 400 μm. The non-thermoresponsive smart windows were prepared with the same size and thickness.

2 Characterizations.

FT-IR measurements were conducted by Spectrum II Li10014 Fourier infrared spectrometer (Perkinelmer, The USA) with a range of 400~4000cm^{-1} and the resolution was 4 cm^{-1}. ATR mode was chosen to perform thermoresponsive changes in the ion gels. The DSC curves of the PBA ion gels were determined on a TA Q2000 differential scanning calorimeter (TA, The USA) with a temperature rate of 3°C/min upon the second heating process from -50 °C to 80 °C. Thermogravimetric analysis (TGA) was performed on a TG209 thermogravimetric analyzer (Netzsch, Germany) to obtain the thermal stability a heating speed of 5°C/min from 50 °C to 700 °C in N_2 atmosphere. Rheology measurements were performed on MCR302 modular intelligent advanced rotary rheometer (Anton Paar, Austria). Temperature sweeps were conducted with a thickness of 100 μm and a diameter of 25 mm at 6.28 rad/s and frequency sweeps were measured in a range of 0.1~100rad/s with 1% strain amplitude at 20°C and 40°C, respectively. Tensile tests were carried out in an Instron 5976 material universal testing machine (Instron Corporation, US) to obtain the mechanical properties of ion gels with a tensile rate was 10mm/min at 25 °C and 50 °C. The size of sample was 50mm×10mm×1mm. Variable temperature compression tests were carried out at a compression rate of 100mm/min with ion gel size of height, 20 mm and diameter, 12 mm. Thermal conductivities (k) were measured on a TC3000E thermal conductivity tester (Xi'an Xiaxi Electronic Technology Co.,Ltd, China) according to ASTM standards, in using a water bath to stabilize the temperature from 25°C to 40°C. The sample size was 40 mm×30 mm×0.8 mm. The water contact angles were characterized by OSA 60 optical surface analyzer (Ningbo NB Scientific Instruments Co., Ltd, China) at 20°C and 50°C, and each test was repeated at least twice to reduce errors. Anti-fogging tests were conducted at ambient with a humidity of 40% after PBA ion gels or ordinary glass being stored at -20 ºC for 30 mins.

3 Measurements

3.1 Transmittance measurements

The transmittance was measured by USB fiber optic spectrometer NBT-4000 (Beijing Niubite Science &Technology Co., Ltd, China) with a hot stage to control temperatures ±0.3°C. The transparent ion gel was places on the hot stage as covered by glasses. The transmittance curves were recorded at a heating rate of 1°C/min or at applied voltages. Each group of samples was tested twice to eliminate errors. For the regulation of whole solar range (180-3000 nm), the transmittance measurements were measured by a 3600 ultraviolet-visible near infrared spectrometer (Shimadzu Corporation, Japan) at temperatures of 25 °C, 30 °C and 35°C. The sample was prepared in a glass cell with a size of 45mm×12.5mm×3.5mm (optical path is 3.5 mm).

The integrated visible transmittance T_{lum} (380-780 nm), infrared transmittance T_{IR} (780-2500 nm) and solar transmittance T_{sol} (380-2500 nm) were calculated by using Equation 1:

$$T_{lum} = \frac{\int \varphi_{lum}(\lambda) T(\lambda) d\lambda}{\int \varphi_{lum}(\lambda) d\lambda} \qquad (Equation\ 1)$$

$$(Equation\ 1）$$

Where T(λ) is the transmittance when the incident light wavelength is λ; φ_{lum}(λ） denotes the standard luminous efficiency function for the photopic vision of human eyes (wavelength coverage of 380-780 nm); $\varphi_{IR/sol}$(λ） is AM 1.0 standard irradiance of infrared/solar spectrum(wavelength coverage of 380-2500 nm).

The visible light modulation efficiency (ΔT_{lum}), infrared modulation efficiency (ΔT_{IR}) and solar light modulation efficiency (ΔT_{sol}) were calculated by using Equation 2:

$$\Delta T_{lum/IR/sol} = T_{lum/IR/sol,\ below\ LCST} - T_{lum/IR/sol,\ above\ LCST} \qquad (Equation\ 2)$$

Where $T_{lum/IR/sol,\ below\ LCST}$ is the transmittance without LCST phase transition; $T_{lum/IR/sol,\ above\ LCST}$ is the transmittance after LCST phase transition occurs.

3.2 Modulated house for thermal managements

Simulated indoor tests used a TY-FL32 xenon light source (Shanghai Standard & Poor's laboratory equipment Co., Ltd, China). A foam made model house (size:14cm

× 14cm × 14cm; thickness: 1cm) was made with a window (size: 5cm × 5cm × 0.2 cm). The outer layer of foam walls was coved by aluminum foil to reduce the thermal exchange with ambient. The temperatures of the ion gel smart window near the light source were defined as T_{out} and other side was T_{in}. The temperature in inside of the house was T_{house}. The xenon light source was 15cm above the chamber to control irradiation intensity of 50W/cm². At the beginning of the test, the xenon lamp was turned on for preheating and stabilizing the surrounding temperatures. Then the model house was placed at the fixed positions to start measurements of each temperature. After reaching thermal steady state, the light source was removed to record the temperature recovery. Each test was repeated three times to reduce errors.

The thermal transmission energy was calculated by Equation 3

$$Q = \int kA\frac{\Delta T(t)}{b}dt \qquad (Equation\ 3)$$

Where k is the thermal conductivity, A and b are the heat transmitted area and length. ΔT is the temperature difference along the time between the conduction lengths.

The thermal absorption of the smart windows was calculated according to Equation 4:

$$Q = \Delta TmC \qquad (Equation\ 4)$$

where Q (kJ/m^3) is thermal energy, ΔT is temperature changes, and C is the heat capacity. Additionally, the energy saving in using ion gel smart windows was also calculated by Equation 4.

3.3 Electrochromic measurements

Electrochromic device was fabricated by spraying PEDOT solution on ITO glasses. The PEDOT solution (PEDOT/PSS 1.5wt% in water) was sprayed on surface of the ITO glass with a coating thickness of 10 μm. In details, the PEDOT solution injected from an airbrush (PULETPU180K, TAIWAN) with an internal diameter of 0.2mm was used to fabricate spray-on thin films. A pressure regulating valve had set the carrier air pressure to be 0.5 MPa before entering into nozzle. The distance from nozzle tip to substrate was kept constant at 100 mm, the lateral nozzle velocity was set at 100 mm/s. The PEDOT coated ITO glasses were then dried to remove solvent

under vacuum.

The conductivity and electrochromic properties of PBA ion gels were characterized using a CHI 760E electrochemical workstation with a temperature controller, assembled by two coating ITO glasses. Electrochemical impedance spectroscopy (EIS) measurements were measured in using the conventional alternating current impedance method and the conductivity (σ) was calculated by using the equation 5:

$$\sigma = d/(R*S) \qquad \text{(Equation 5)}$$

where d, *R*, and S are the thickness, resistance, and upper surface area of the sample, respectively.

3.4 Ionic thermoelectric measurements

The Thermal voltage was measured by a keithley voltmeter. The size of ion gel was 2cm×1cm×0.2cm. One side was placed on the WT-3000-12S precision constant temperature working heating table (Shanghai Weitu Instrument Technology Development Co.,Ltd, China), and the other side was exposed to the air, the two wires of the galvanometer were respectively connected to the heated side and the other side of the ion gel as shown in Figure S10. The temperature of the hot stage rose from 25°C to 75°C with a temperature interval of 10°C. The dimensionless figure of merit (ZT) related to the thermoelectrical device properties was calculated according by

$$ZT = S_e^2 \cdot \sigma \cdot T/k \qquad (Equation\ 6)$$

where S_e is seeback coefficient, σ resembled ionic conductivities, and k is thermal conduction coefficient.[1]

3.5 Self-defensive tests

The impact test was performed by using a steel ball with a diameter of 30 mm and a mass of 125 g for free fall onto various substrates: PBA ion gels, ordinary glass, and ITO glass. Before the experiments, these substrates were fixed at the end of the transparent circular tube, and the small steel ball was placed at the beginning of the transparent circular tube to make the free fall. For the impact resistance test of iron ball, a free-falling impactor, h was obtained until the iron ball broke the samples. The impact resistance for specific energy absorption is calculated by

$$E = (mv_0^2)/2d\rho \qquad \text{(Equation 7)}$$

where m is the mass of iron ball, d is the thickness of sample, ρ is the density of sample and v_0 is the velocity of iron ball touching sample. The velocity of iron ball just touching sample was calculated by free-fall formula, $v_0 = (2hg)^{1/2}$, where h is the free-fall distance (m) and g is the acceleration of gravity (9.8 m s^{-2}). This was repeated several times for each material.

4 Figures

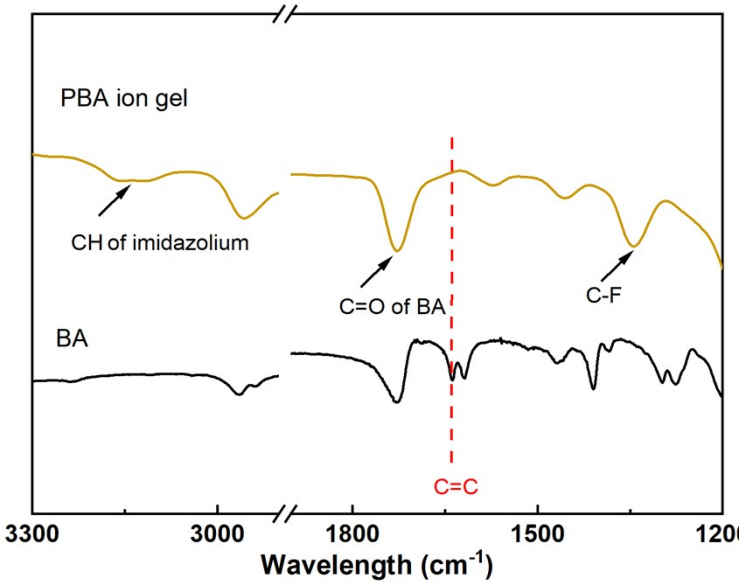

Figure S1 FT-IR spectra of BA and PBA ion gel

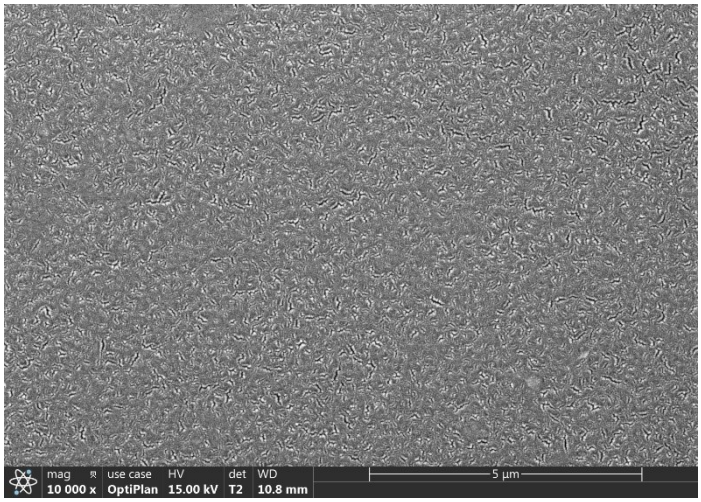

Figure S2 SEM pictures of the PBA ion gels.

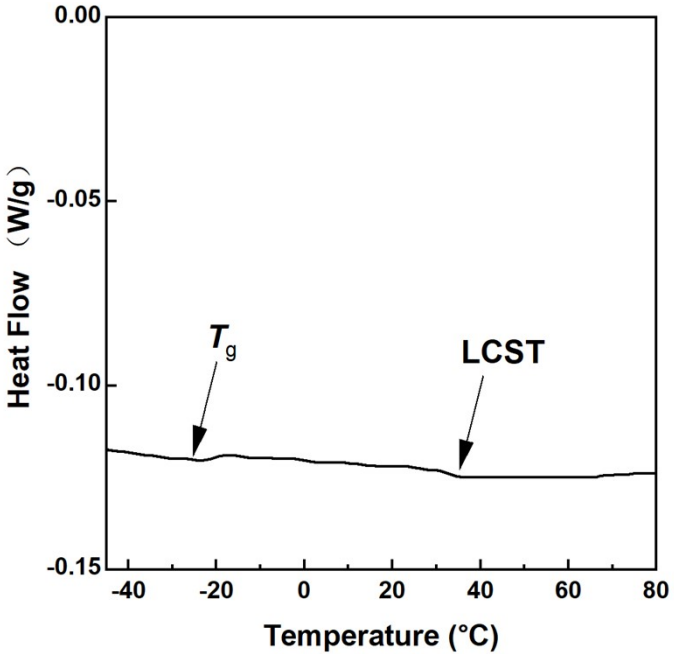

Figure S3 DSC curves of the PBA ion gels upon heating process at a speed of 3ºC/min.

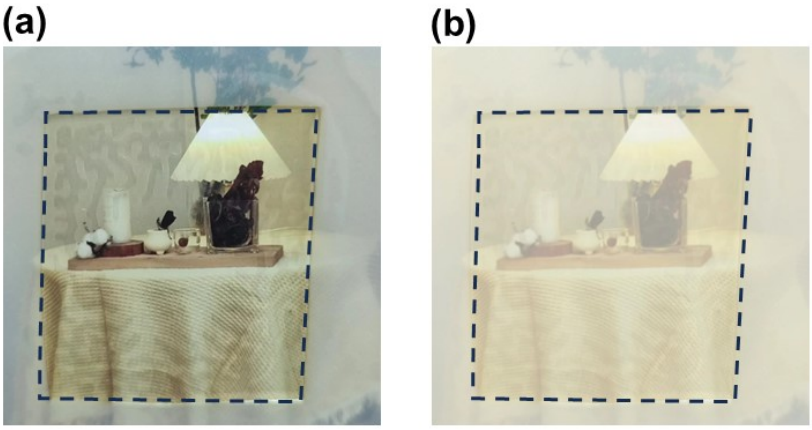

Figure S4 Size changes of the PBA ion gel before (a) and after LCST behaviors(b).

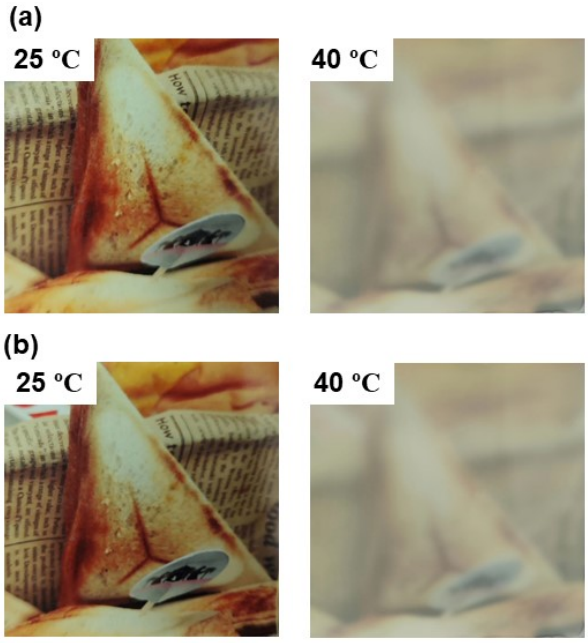

Figure S5 Optical pictures of the PBA ion gels at 25 and 40 ºC in fresh states (a) and after being stored for 2 years.

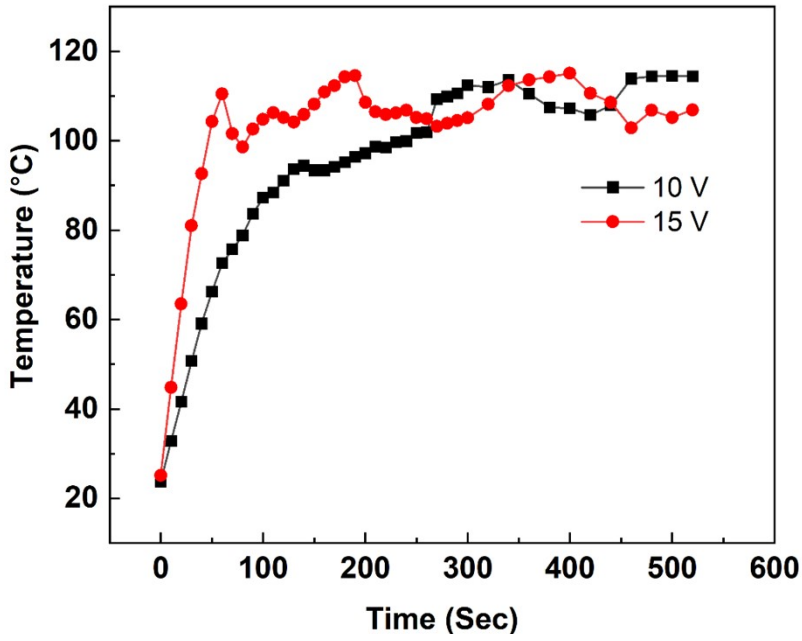

Figure S6 Temperature changes of conductive ITO glasses with a voltage of 10 V and 15 V, respectively.

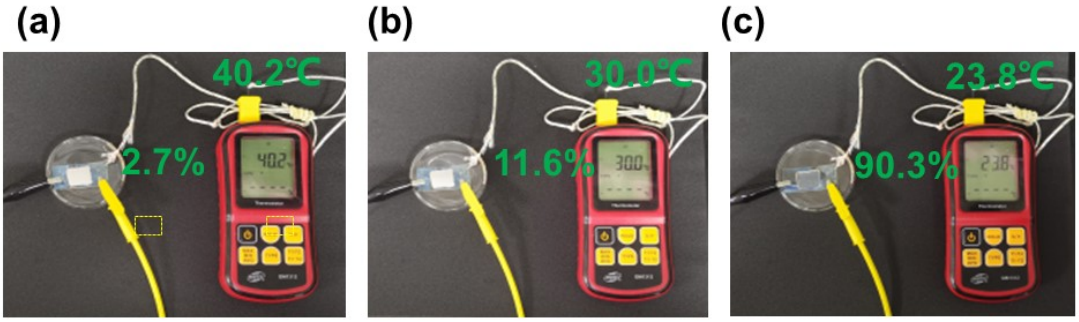

Figure S7 Recovery of the PBA ion gels upon cooling process. Left words in green color means transmittance values and the right side means the alive temperature of ion gels after removing voltages.

Figure S8 Photograph of model house in using PBA ion gels as smart windows.

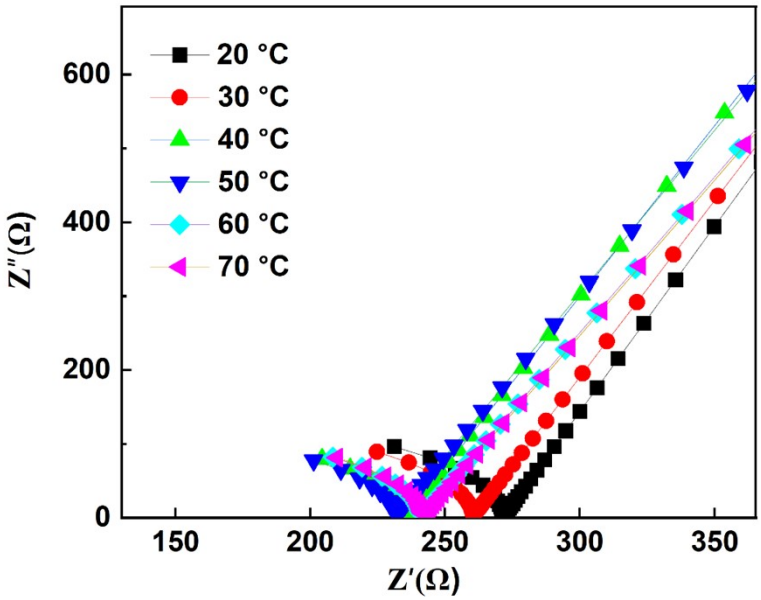

Figure S9 Nyquist plots of the ITO assembled PBA ion gels upon heating process.

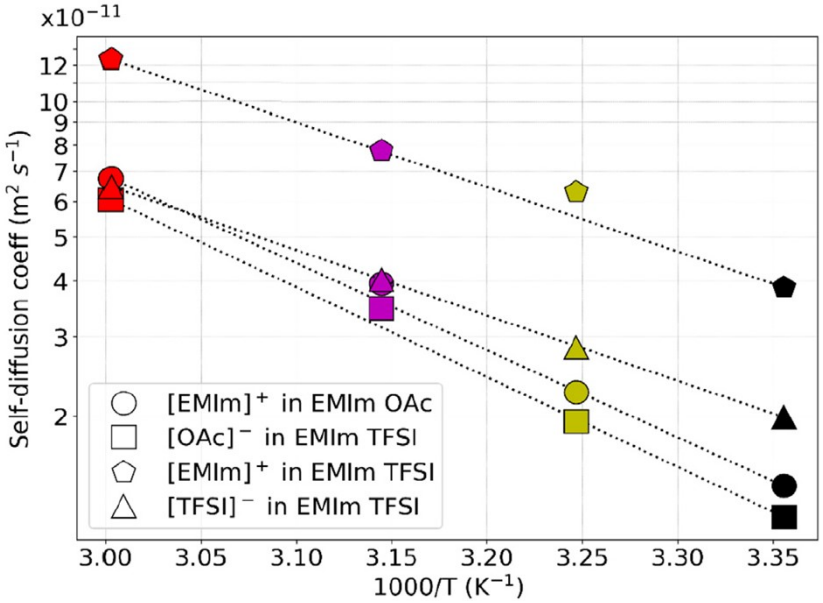

Figure S10 Arrhenius plot of self-diffusion coefficients of the individual ions in the temperature ranges for the ionic liquids C_2mim[Ntf_2] as reported in picture: EMIm TFSI. [2]

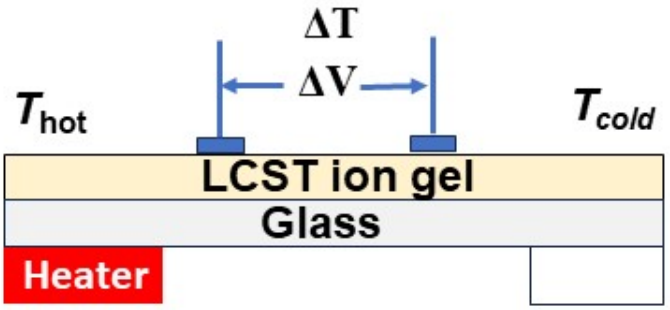

Figure S11 A measurement illustration of thermo-induced voltages for the PBA ion gels between T_{hot} and T_{cold}.

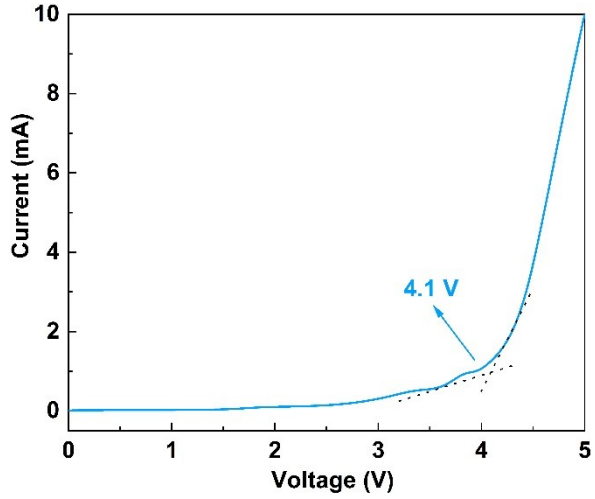

Figure S12 Cyclic voltammetry curves for PBA ion gels at a scanning rate of 10 mV/s.

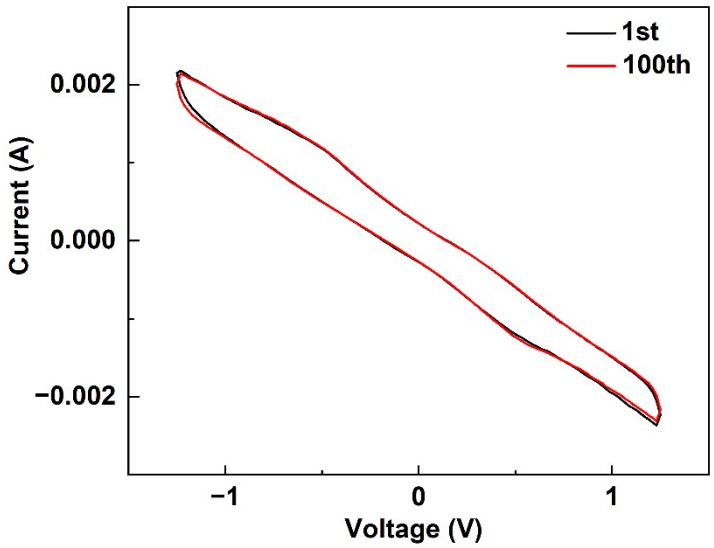

Figure S13 CV curves in 100 cycles of PBA ion gels at a scanning rate of 10 mV/s at 25 ºC.

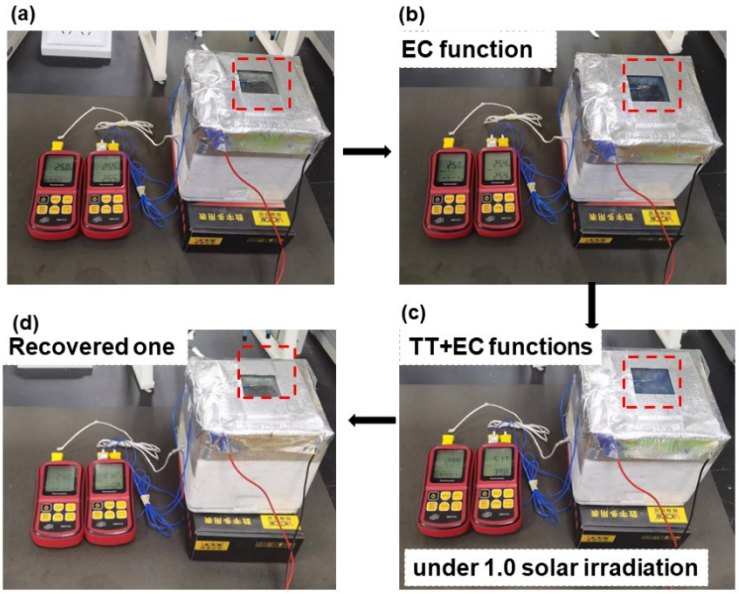

Figure S14 Pictures of PBA ion gel assembled windows in different working modes: normal one (a), and switching EC function on (b), switching EC and TT functions on (c) and recovered one after removing voltage and 1.0 solar irradiations(d).

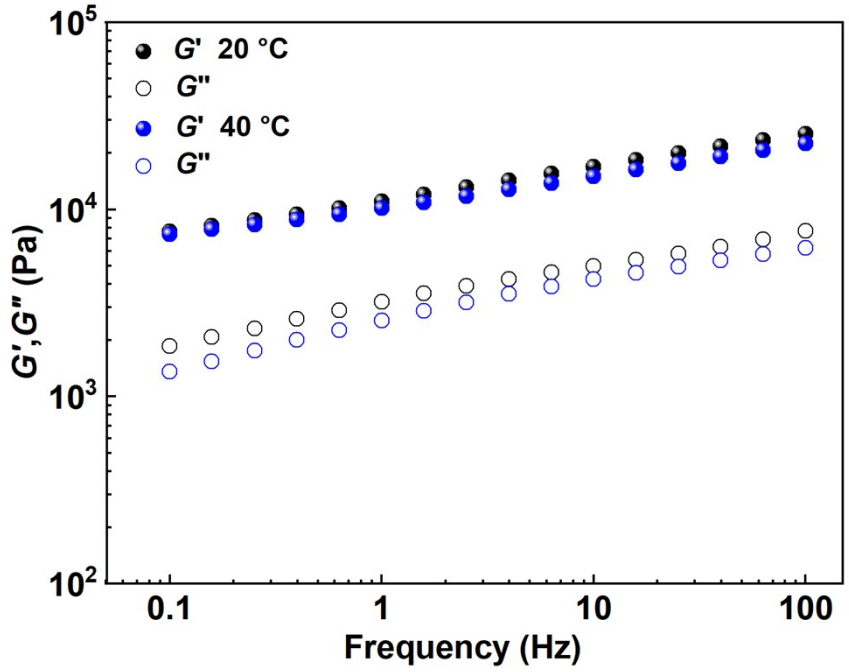

Figure S15 Frequency sweeps of PBA ion gels with a strain of 1 % at 20 and 40 ºC.

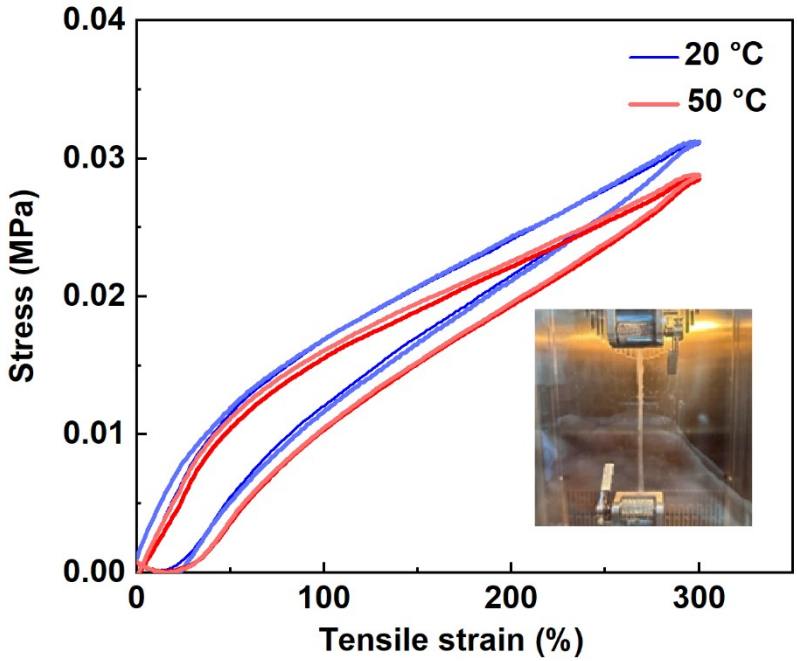

Figure S16 Alternated stretching curve of ionic gel at 20 ºC (blue line) and 50 ºC (red line) respectively, and inserted picture is the stretched ion gel at 50 ºC.

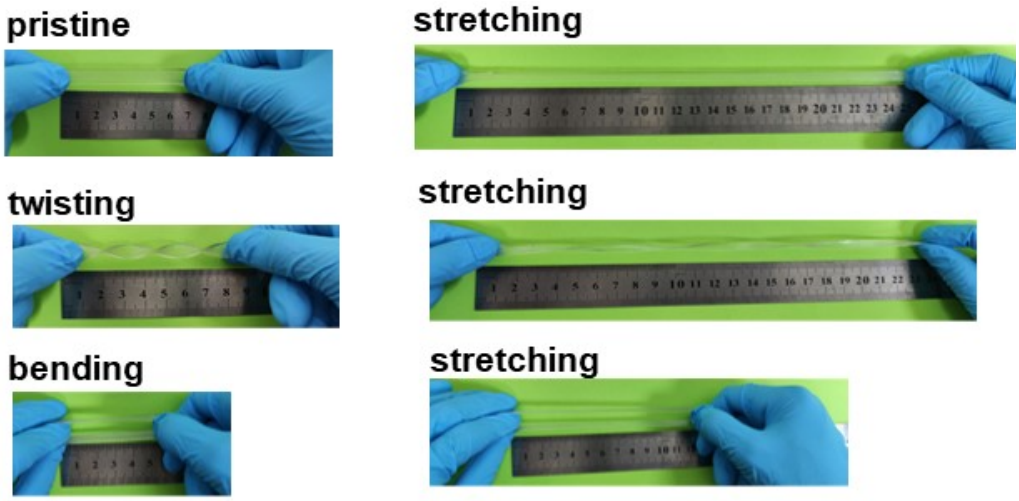

Figure S17 Photographs of the PBA ion gels showing their ability to withstand stretching, bending, and twisting.

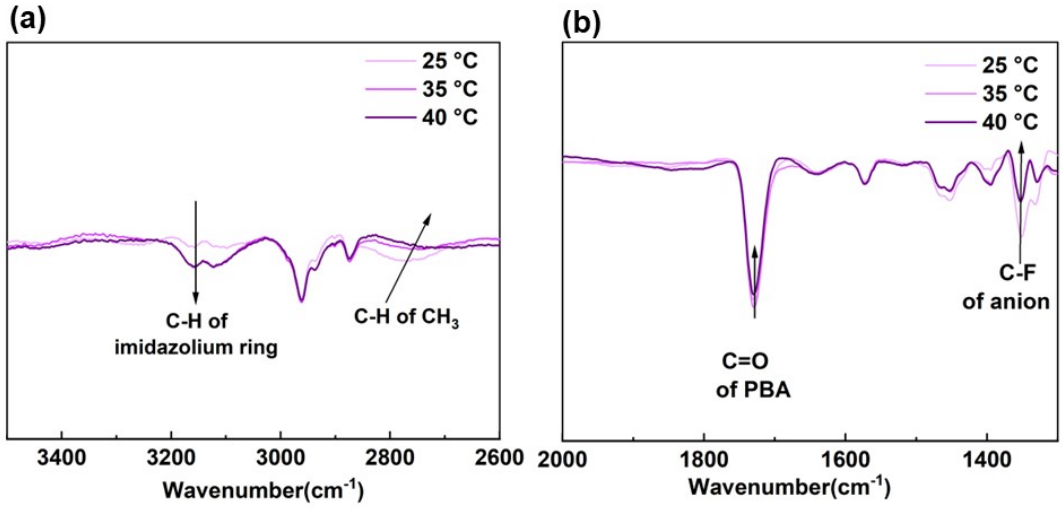

Figure S18 FT-IR spectra of PBA ion gels upon heating process at C-H range of imidazolium cations(a) and C=O region of the polymers and C-F region of the anion(b).

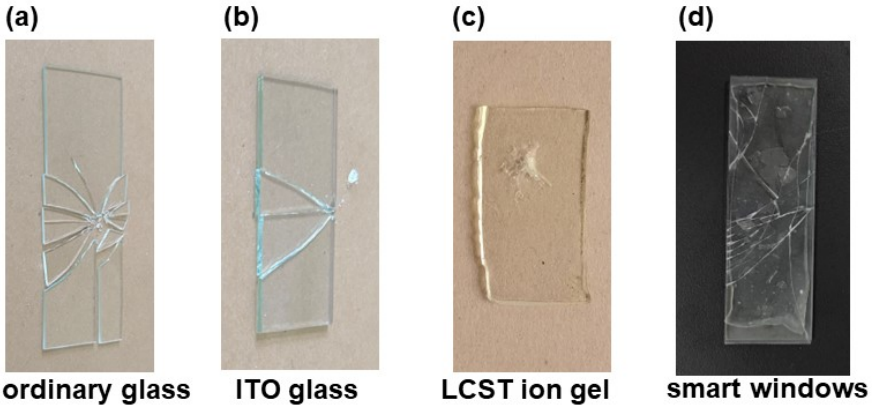

Figure S19 Broken pieces of ordinary glass, ITO glass, LCST ion gel and smart windows after free fall of 125 g iron ball from 3 cm (a), 2 cm (b), 150 cm(c) and 100 cm (d).

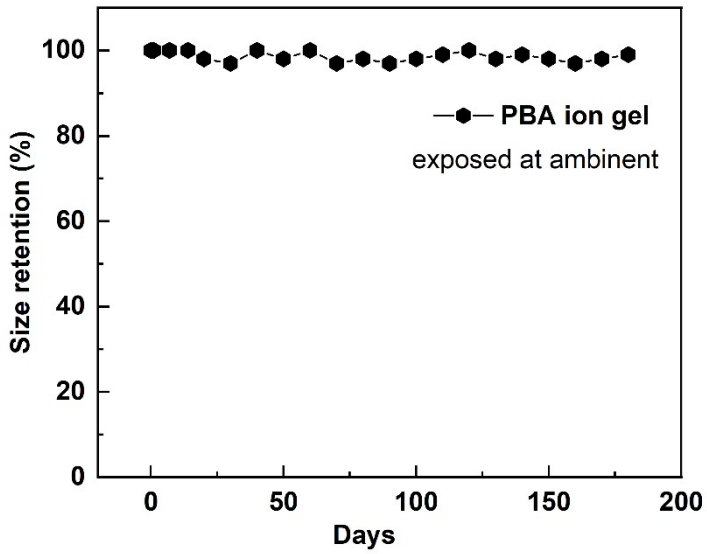

Figure S20 Size retention of the PBA ion gels for over 180 days in an exposed ambient, Chengdu.

5 Tables

Table S1 Optical performances for the LCST ion gels under solar illuminations upon heating process.

Temperature(℃)	T_{lum}[%]	ΔT_{lum}[%]	T_{IR}[%]	ΔT_{IR}[%]	T_{sol}[%]	ΔT_{sol}[%]
25	83.67	0	79.63	0	81.63	0
30	64.06	19.61	75.35	4.28	68.99	12.63
35	7.47	76.20	42.97	36.66	24.52	57.11

Table S2 Comparison of smart window properties with reported literatures.

Devices	Preparation method	Responsive temperatures	Optical property	Function	Refs
LCST Ion Gels As "all-in-one" Smart Window	In situ polymerization	28ºC	ΔT_{sol} 57.1% ΔT_{lum}76.2% 7s	TC+EC+PG	This work
Cellulose-based alcogel	complicated	60ºC	ΔT_{sol} ~80%, 8s	TC+ self-defensive	3
LCST ion gel	*in situ* polymerization	60ºC	ΔT_{sol} 72% 8 s	TC	4
LCST ion gel	*in situ* polymerization	35 ºC	ΔT_{sol} 89.1%	TC+EC	5
PiPO-POE hydrogel	Facile	59 °C	ΔT_{sol} 75% 11s	TC+EC	6
PNIPAm hydrogel	Radical polymerization and casting	32°C	ΔT_{sol} 70.8% 10s	TC	7
VO_2/hydrogel	*in situ* polymerization	68°C	ΔT_{sol} 35% -	TC	8
$MAPbI_{3-x}Cl_x$ thermochromic perovskite	complicated	51 °C	ΔT_{sol} 23.7% (1–4 min)	TC+PG (Perovskite cell)	9

Table S3 Comparison of ionic thermoelectric properties of ionic conductors.

	σ(mS/cm)	Se (mV/ K)	*k* (W/ (m· K))	*ZT*	*Refs*
PEO/NaOH	0.0813	11.1	0.216	$1.38*10^{-3}$	[10]
TBAN-dodecanol	0.012	7.16	0.17	$1.1*10^{-4}$	[11]
EMIM-DCA/PVDF-HFP	6.7	26.1	0.176	0.75	[12]
This work	0.3	2.6	0.16	0.022	

References

1 X. He, H. Cheng, S. Yue and J. Ouyang, *J. Mater. Chem. A*, 2020, **8**, 10813–10821.

2 M. Haque, I. Abdurrokhman, A. Idström, Q. Li, A. Rajaras, A. Martinelli, L. Evenäs, P. Lundgren and P. Enoksson, *Electrochim. Acta*, 2022, **403**, 139640.

3 S. Chen, G. Jiang, J. Zhou, G. Wang, Y. Zhu, W. Cheng, G. Xu, D. Zhao and H. Yu, *Adv. Funct. Mater.*, 2023, **33**, 2214382.

4 S. Dai, X. Dong, Y. Jiang, J. Ge, J. Ding and N. Yuan, *ACS Appl. Polym. Mater.*, 2023, **5**, 3398–3404.

5 H. Wu, M. Wang, W. Wu, D. Bai, Y. Liang, S. Hu, W. Yu, P. He and J. Zhang, *J. Mater. Chem. A*, 2023, **11**, 9626–9634.

6 J. M. C. Puguan, P. V. Rathod and H. Kim, *Adv. Opt. Mater.*, 2023, **11**, 2201773.

7 G. Li, J. Chen, Z. Yan, S. Wang, Y. Ke, W. Luo, H. Ma, J. Guan and Y. Long, *Mater. Horizons*, 2023, **10**, 2004–2012.

8 Y. Zhou, Y. Cai, X. Hu and Y. Long, *J. Mater. Chem. A*, 2015, **3**, 1121–1126.

9 S. Liu, Y. W. Du, C. Y. Tso, H. H. Lee, R. Cheng, S. P. Feng and K. M. Yu, *Adv. Funct. Mater.*, 2021, **31**, 2010426.

10 D. Zhao, H. Wang, Z. U. Khan, J. C. Chen, R. Gabrielsson, M. P. Jonsson, M. Berggren and X. Crispin, *Energy Environ. Sci.*, 2016, **9**, 1450–1457.

11 H. Wang, D. Zhao, Z. U. Khan, S. Puzinas, M. P. Jonsson, M. Berggren and X. Crispin, *Adv. Electron. Mater.*, 2017, **3**, 1700013.

12 H. Cheng, X. He, Z. Fan and J. Ouyang, *Adv. Energy Mater.*, 2019, **9**, 1901085.